DYNAMIC ANALYSIS OF A MAGNETIC BEARING SYSTEM WITH FLUX CONTROL

Josiah Knight

Thomas Walsh

Lawrence Virgin

Department of Mechanical Engineering
and Materials Science
Duke University
Durham, NC

SUMMARY

Using measured values of two-dimensional forces in a magnetic actuator, equations of motion for an active magnetic bearing are presented. The presence of geometric coupling between coordinate directions causes the equations of motion to be nonlinear. Two methods are used to examine the unbalance response of the system: simulation by direct integration in time; and determination of approximate steady state solutions by harmonic balance. For relatively large values of the derivative control coefficient, the system behaves in an essentially linear manner, but for lower values of this parameter, or for higher values of the coupling coefficient, the response shows a split of amplitudes in the two principal directions. This bifurcation is sensitive to initial conditions. The harmonic balance solution shows that the separation of amplitudes actually corresponds to a change in stability of multiple coexisting solutions.

INTRODUCTION

In the short time since the introduction of practical magnetic levitation for rotating shafts, significant progress has been made in designing and modelling the performance of magnetic bearings, to the point where they are practical for a variety of applications. These include machine tool spindles, pumps, compressors, gyroscopes and momentum wheels [1]. Some applications, those with significant rotor flexibility and coordinate cross coupling, present difficult challenges, however. In this category fall some pumps and many compressors and turbines, including gas turbines. Recent papers, such as those of Williams, et al. [2], Lee and Kim [3], and Nonami , et al.[4] have confronted limitations of vibration control at high speeds for flexible rotors using magnetic bearings. Rotor dynamic stability and robust vibration control in these machines will increasingly depend on an understanding of the system dynamics that goes beyond traditional linear models.

This paper presents equations of motion and simulations of a two-degree-of-freedom system subject to forces from an actively controlled magnetic actuator, where the control is linear but the forces from the actuator include coordinate coupling of a form found in experimental measurements. The resulting equations are nonlinear and coordinate-coupled, and the response contains several features found only in nonlinear systems.

ACTUATOR FORCES

A schematic of an active magnetic bearing is shown in Figure 1. It consists of two opposed pairs of electromagnets arranged around a shaft. Each of the magnet pairs will be controlled independently. The control is linear, taking as input the shaft displacement along the

axis of the magnet pair, and producing as output a variation of the magnetic flux B. This type of control is an idealization from the practical case, where control is more easily exerted on either the current or the voltage applied to the magnet coils.
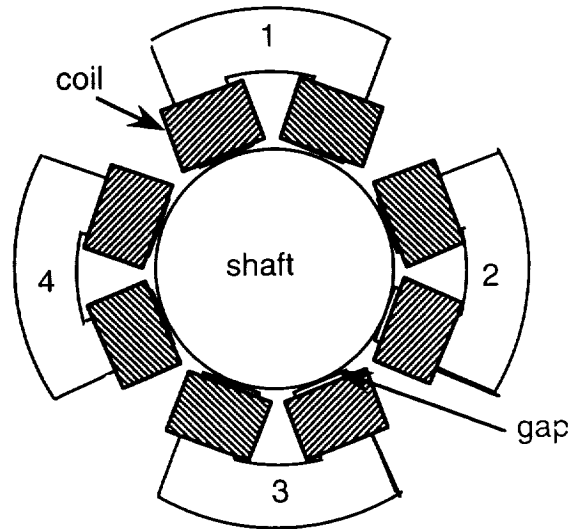
Figure 1. Magnetic bearing actuator. Sensors and control not shown.

The force between a magnet and a ferromagnetic part is the negative of the derivative of magnetic field energy with respect to virtual displacement of the part. The traditional model for forces from a magnetic actuator in a magnetic bearing is based on one-dimensional magnetic circuit theory, in which it is assumed that the lines of magnetic flux cross the air gaps of the bearing in straight lines. It is generally assumed that the direction of the force is along the axis of symmetry of the magnet. In a previous paper [5] measurements were described in which the forces from a magnet with curved pole faces acting on a circular shaft had both an attractive component and a component normal to the axis of the magnet when the shaft was given a displacement away from this symmetry axis. The ratio of forces was found approximately proportional to the normal coordinate.

In the calculations that follow, both principal forces and normal forces are assumed to act. The principal force from each magnet is modelled by this one-dimensional circuit theory, in which

$$F_p = \frac{aB^2}{\mu_0}$$ (1)

where
a = pole cross section area
B = magnetic flux

μ_0 = permeability of free space

Often the flux is written as a function of the coil current i, wire turns N and gap h, leading to

$$F_p = \frac{\mu_0(Ni)^2 a}{4h^2}$$ (1a)

354

In the present work, the controlled quantity is assumed to be the flux B, so Equation (1) will be used to model the attractive force between each magnet and the shaft

Based on the measurements of [5], the normal force is considered to be

$$F_n = \alpha F_p \qquad (2)$$

where the coupling parameter α is empirical. The directions p,n correspond to directions x,y or y,x as appropriate for each magnet.

Linear Flux Control

Consider the case in which a point mass is acted on by two opposed magnet pairs, shown schematically in Figure 1. In an attempt to linearize the system so that the mass effectively is subject to a linear restoring force like a spring stiffness, a large bias flux B_b is introduced in each magnet gap, and a control flux B_c is superposed. If the bias flux is equal in both magnets of the vertically oriented pair

$$B_{1b} = B_{3b} = B_b \qquad (3)$$

This constitutes the special case in which the bearing is not required to support a steady load, as in a vertically oriented machine.

If the control flux is made equal in magnitude but opposite in sign in the two magnets

$$B_{1c} = -B_{3c} = B_c \qquad (4)$$

then the resultant force in the y direction

$$F_{y\,(1,3)} = \frac{a}{\mu_o}\left[(B_{1b} + B_{1c})^2 - (B_{3b} + B_{3c})^2\right] \qquad (5)$$

is linear in the control flux

$$F_{y\,(1,3)} = \frac{4a}{\mu_o} B_b B_c \qquad (6)$$

Coordinate Coupling

The approach above ignores the normal force found by experiment and calculation. This normal force results in the need for control in the x direction as well. Suppose that an additional magnet pair is placed on the x axis, subject to the same bias and control flux as the y-direction pair. For instance, let the control flux in each magnet be proportional only to the distance from that magnet, neglecting for the present any derivative control. That is

$$B_c = -\kappa B_b x_p \qquad (7)$$

where the subscript p denotes the principal axis, the axis of symmetry of the magnet.

Then, adding all the forces in the x direction

$$F_x = \frac{-4aB_b^2}{\mu_o}\left[\kappa x - \frac{\alpha}{2}x\left(1 + \kappa^2 y^2\right)\right] \tag{8}$$

Similarly, the y direction force is

$$F_y = \frac{-4aB_b^2}{\mu_o}\left[\kappa y - \frac{\alpha}{2}y\left(1 + \kappa^2 x^2\right)\right] \tag{9}$$

It is seen that the coordinate coupling embodied in the parameter α has two effects: it obviously yields a force normal to the displacement, but it also attenuates the restoring force, reducing the effective stiffness. Both these effects occur even though the independent-axis control algorithm is assumed perfect in its ability to give a linear stiffness characteristic in the principal direction.

The forces given by Equations (8) and (9) are derivable from a potential energy function

$$v = \frac{4aB_b^2}{\mu_o}\left[\left(\frac{\kappa}{2} - \frac{\alpha}{4}\right)\left(x^2 + y^2\right) - \frac{\alpha}{4}\kappa^2 x^2 y^2\right] \tag{10}$$

This quantity may be rendered dimensionless

$$V = \left(\frac{K}{2} - \frac{A}{4}\right)\left(X^2 + Y^2\right) - \frac{A}{4}K^2 X^2 Y^2 \tag{10a}$$

using the parameters

$$K = \kappa c \qquad\qquad A = \alpha c$$

$$X = x/c \qquad\qquad Y = y/c$$

$$\tag{11}$$

$$V = v \frac{\mu_o}{4aB_b^2 c}$$

Figure 2 contains plots of the dimensionless potential energy at different levels of the coupling parameter A [6]. The attenuation of principal stiffness with increasing A is evidenced by the decrease in amplitude of the potential, and the normal forces are evidenced by the tendency of the potential surface to sag along lines at 45° to the principal axes. One way to consider the implications of these plots is to visualize them as solid surfaces upon which a mass in the shape of a small sphere might roll if given an initial velocity and/or displacement from the origin. This is a physical analog to the free vibration of a mass subject to the force equations given above.
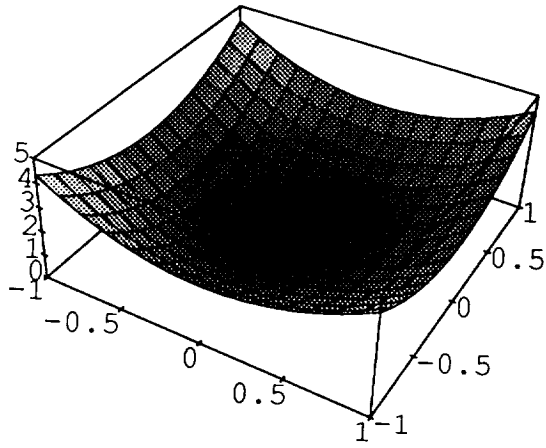
K=5, A=0.1
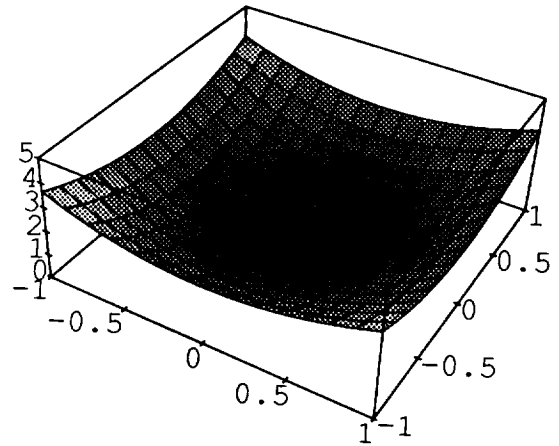
K=5, A=0.2
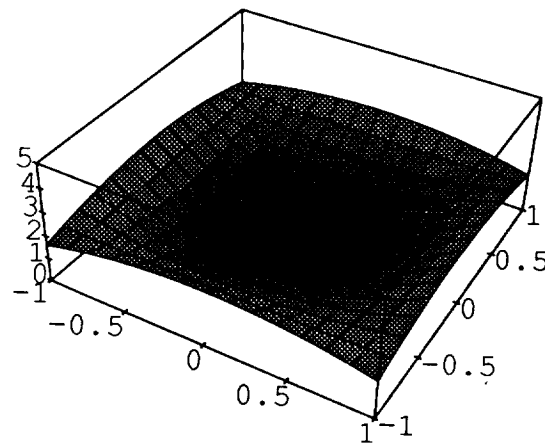
K=5, A=0.5

Figure 2. Potential energy for different degrees of coupling.

If a derivative feedback is added to the proportional feedback

$$B_c = - \kappa B_b x_p - \gamma B_b \dot{x}_p \qquad (12)$$

the force equations

$$F_x = \frac{2aB_b^2}{\mu_o}\left[-2\kappa x + \alpha x\left(1 + \kappa^2 y^2\right)\right] - 2\gamma \dot{x} + 2\alpha\kappa\gamma x y\dot{y} + \alpha\gamma^2 x\dot{y}^2 \qquad (13)$$

$$F_y = \frac{2aB_b^2}{\mu_o}\left[-2\kappa y + \alpha y\left(1 + \kappa^2 x^2\right)\right] - 2\gamma \dot{y} + 2\alpha\kappa\gamma y x\dot{x} + \alpha\gamma^2 y\dot{x}^2 \qquad (14)$$

show a coupling of the proportional and derivative terms in each coordinate, as well as a coupling of both these terms to the other position coordinate.

Consider a mass m subject to the above actuator forces in addition to an unbalance forcing function. Newton's second law is written for each of the coordinate directions, with the resulting equation of motion in x as

$$m\ddot{x} = \frac{-4aB_b^2}{\mu_o}\left[\kappa x - \frac{\alpha}{2}x\left(1 + \kappa^2 y^2\right) + \gamma\dot{x} - \alpha\kappa\gamma x y\dot{y} - \frac{1}{2}\alpha\gamma^2 x\dot{y}^2\right] + m e\omega^2\cos\omega t \qquad (15)$$

or

$$m\ddot{x} = \frac{-4aB_b^2}{\mu_o}\left[\kappa x + \gamma\dot{x} - \frac{\alpha}{2}x\left(1 + \kappa^2 y^2 + \alpha\kappa\gamma y\dot{y} + \frac{1}{2}\alpha\gamma^2\dot{y}^2\right)\right] + m e\omega^2\cos\omega t \qquad (16)$$

and in y

$$m\ddot{y} = \frac{-4aB_b^2}{\mu_o}\left[\kappa y + \gamma\dot{y} - \frac{\alpha}{2}y\left(1 + \kappa^2 x^2 + \alpha\kappa\gamma x\dot{x} + \frac{1}{2}\alpha\gamma^2\dot{x}^2\right)\right] + m e\omega^2\sin\omega t \qquad (17)$$

By choosing the additional nondimensional parameters

$$K = \kappa/c \qquad\qquad E = e/c$$

$$T = t\omega_n \qquad\qquad \Gamma = \gamma c\omega_n$$

$$\Omega = \omega/\omega_n \qquad \omega_n = \sqrt{\frac{4a\kappa B_b^2}{m\mu_o}} \qquad (18)$$

the system of equations can be nondimensionalized. Here, ω_n is the natural frequency the system would have if there were no coupling present ($\alpha = 0$). As Equation (10) indicates, for any positive value of α, the actual natural frequency will be reduced from this value.

The nondimensional forms of the equations are

$$X'' = -\frac{1}{K}\left(KX + \Gamma X' - \frac{A}{2}X\left(1 + K^2Y^2 + 2K\Gamma YY' + \Gamma^2Y'^2 \right) \right) + E\Omega^2\cos\Omega T \quad (19)$$

$$Y'' = -\frac{1}{K}\left(KY + \Gamma Y' - \frac{A}{2}Y\left(1 + K^2X^2 + 2K\Gamma XX' + \Gamma^2X'^2 \right) \right) + E\Omega^2\sin\Omega T \quad (20)$$

where ' and " indicate differentiation with respect to dimensionless time T. These equations may be integrated in time after assigning values to the system parameters K, Γ, A and E, along with appropriate initial conditions for all of the quantities X, Y, X' and Y'. It should also be noted that the forms of the forcing function in the final terms of Equations (19) and (20) also constitute initial conditions, in the form of an assumed phase angle for the forcing function at T = 0.

ANALYSIS

Two methods are used to examine the response of the system to unbalance forcing: numerical integration from arbitrary initial conditions using a fourth-order Runge-Kutta algorithm; and approximate calculation of steady state solutions by the harmonic balance method.

Natural Frequency

Because the potential energy of the system as shown in Figure 2 is not described by a surface of revolution, the natural frequency of the system depends on the initial conditions. If initial conditions of finite displacements and zero velocities are chosen, the period of oscillation in free vibration is a function of the displacements, or alternatively, of the radius and angle of the initial conditions. Figure 3 indicates this dependence. The results were obtained by direct numerical integration, and dissipation was not included. Part (a) shows the period as a function of radius for a fixed angle from the x-axis (22.5°) and part (b) shows the effect of the angle of the initial condition for a fixed radius (0.5). The two periods both increase with radius, a characteristic of systems with softening stiffness. The period in Y is different from that in X because the path of the oscillation does not in general pass through the origin. There is a single period only when the initial conditions lie along a line at 45° to the two axes, as shown in Figure 3b.

(a) Fixed angle from x axis   (b) Fixed radius
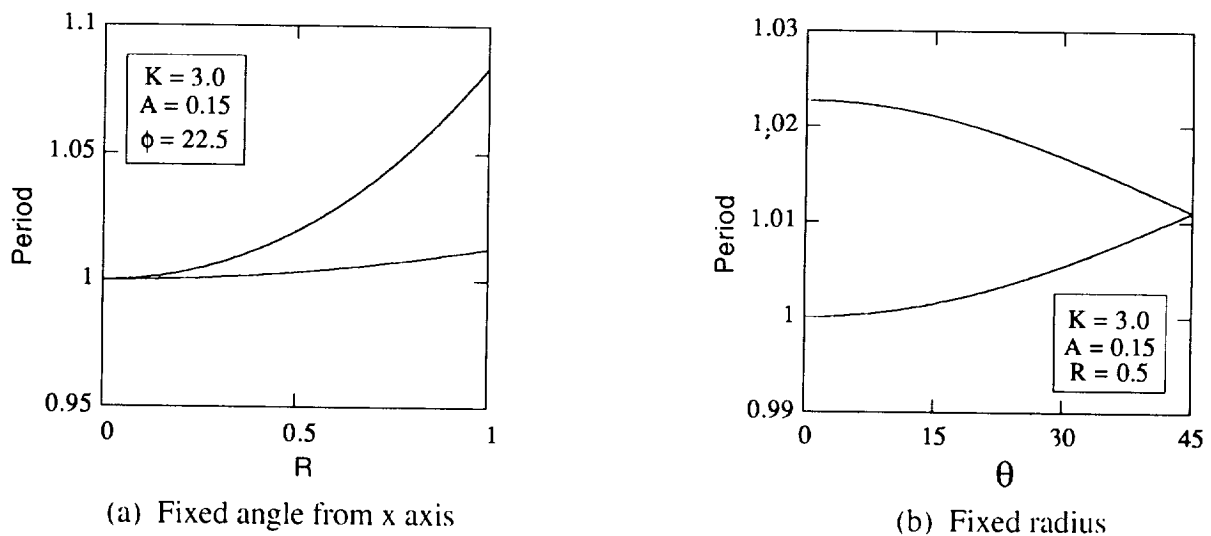
Figure 3. Effect of Initial Conditions on Natural Period

When the derivative control coefficient Γ is made finite so the system dissipates energy, the response of the system to unbalance forcing can be calculated. The effects of three parameters are examined: K, Γ, and A.

The proportional control coefficient K determines how rapidly the flux, and thereby the force, from a magnet is reduced as the shaft approaches that magnet. A value of K=1 would cause the flux to be reduced to zero at contact (not counting the contribution from the derivative control coefficient Γ). Larger values of K would correspond to "stiffer" bearings. Because of the form of nondimensionalization of Equations (19) and (20), however, an increase in K while holding Γ constant causes a decrease in the effective dissipation coefficient, by virtue of a change in the natural frequency. This must be considered when interpreting the results of parametric studies, since a straightforward increase in the dimensional quantity κ (1/m) would not affect the dissipation, or derivative control, coefficient. The fact that K cannot be eliminated from the equations of motion is a result of the essential nature of nonlinear systems.

The measurements of [5] indicate that A=0.15 is a reasonable value for the coordinate coupling coefficient A. In the calculations below, A is varied from 0.05 to 0.25.The values of Γ were chosen to provide dissipation of the same order as in a linear system having damping ratios between 0.1 and 0.3 . In all the results presented here, the unbalance magnitude is E=0.1 .

Studies examining large ranges of parameter combinations are planned but are beyond the scope of the present work. Nevertheless, much can be learned from a limited parametric study.

Figure 4 shows the effect of increasing the coefficient K from 1.0 in part a to 3.0 in part b to 5.0 in part c. As noted above, increasing K alone results in a smaller value of the derivative control coefficient. With this in mind, Figure 4 still indicates an important feature of the system: that for some combinations of parameters, the response exhibits a split, with the motion on one axis having a much higher amplitude than that on the other axis. Associated with this split is a sudden jump in one of the amplitudes as the frequency is increased. In fact, one of the solutions of Figure 4c extends beyond an eccentricity of 1.0, which in the physical case would result in solid contact. At some frequencies near the natural frequency, however, two solutions exist that are both within the physical bounds of the system. Furthermore, the solutions are dependent on the initial conditions. For the case shown, the integration begins with both shaft position and velocity equal to zero. The numerical integration proceeds until all transients have decayed and the peak amplitudes in the two directions are sampled. The forcing function, the final terms in Equations (19) and (20), also imposes an implicit initial condition by virtue of its assumed phase. In fact, the cosine portion of the forcing function begins with a step imposition of force at time t=0, although all transients associated with this discontinuity have decayed before the amplitudes are sampled. If, however, the cosine and sine parts of the force are exchanged, the solutions for X and Y are also found to have exchanged places. This is in marked contrast to a linear system, where the amplitude is unique after transients have decayed.
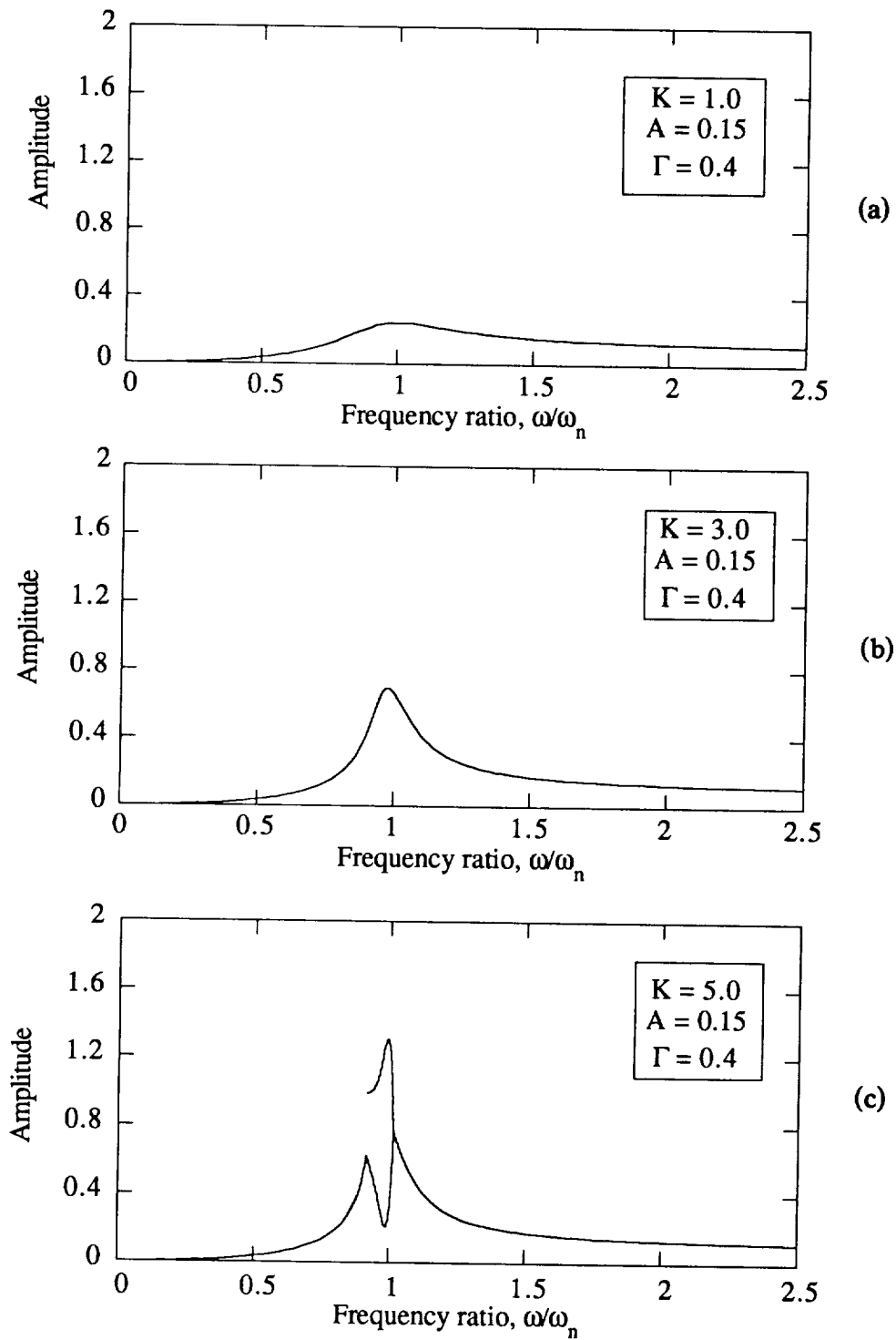
Figure 4. Effect of variation in dimensionless proportional control coefficient K.

The effect of the coupling parameter can also be examined. Figure 5 illustrates the effect of increasing the value of A, while K is held constant at 0.3. The values of all parameters except A are equal to those of the case shown in Figure 4b. As A is increased beyond a threshold value, between 0.15 and 0.25, multiple solutions appear near the natural frequency. In this set of plots, the natural frequency is a constant, making this parametric variation somewhat easier to interpret than the previous one.

Reduction of the derivative control coefficient Γ can also bring about a situation with multiple solutions, as shown in Figure 6, as can an increase of the unbalance eccentricity, not shown.

Thus, the bifurcation seems mostly to be an amplitude-driven phenomenon, such that when a critical amplitude is exceeded, the solutions split. In all cases, the split is initial-condition-dependent.

Solution by Harmonic Balance

Another approach to examining the steady-state response of a nonlinear system is the harmonic balance method, which is approximate but analytical rather than numerical. It has the advantage that both stable and unstable solutions can be located, whereas numerical integration can locate only stable solutions.

The method consists of assuming steady solutions of the form

$$X = C \cos\Omega T + D\sin\Omega T \tag{21}$$

$$Y = G \cos\Omega T + H\sin\Omega T \tag{22}$$

where C, D, G, and H are to be determined. Equations (21) and (22) are differentiated and substituted into the equations of motion. The resulting powers of trigonometric functions are expanded using trig identities, after which the harmonics higher than 1 are neglected. Because the truncation of higher harmonics is not performed until after the powers of trig functions are expanded, the solution retains its nonlinear character, although the equations have been approximated. The resulting four algebraic equations for the constants C, D, G, and H are coupled and highly nonlinear and must themselves be solved by a numerical Newton-Raphson iteration [6]. When the constants are found, the steady amplitudes can be calculated readily.

Figure 7 shows the amplitudes obtained by harmonic balance for the case corresponding to Figure 5a. These results indicate that in the neighborhood of the natural frequency, four solutions actually exist. (Two are identical.) Two of the solutions are apparently unstable, but the harmonic balance method does not yield stability characteristics. Based on the results of numerical integration, however, it appears that the solutions corresponding to equal amplitudes for X and Y are unstable when they lie between the unequal solutions. Thus the jump in one of the amplitudes stems from a change in that solution's stability. Where the equal-amplitude solutions lie below the unequal solutions, they are the stable ones. The unequal solutions are believed to exist at all frequencies, but are difficult to locate by Newton-Raphson beyond the range that is shown.
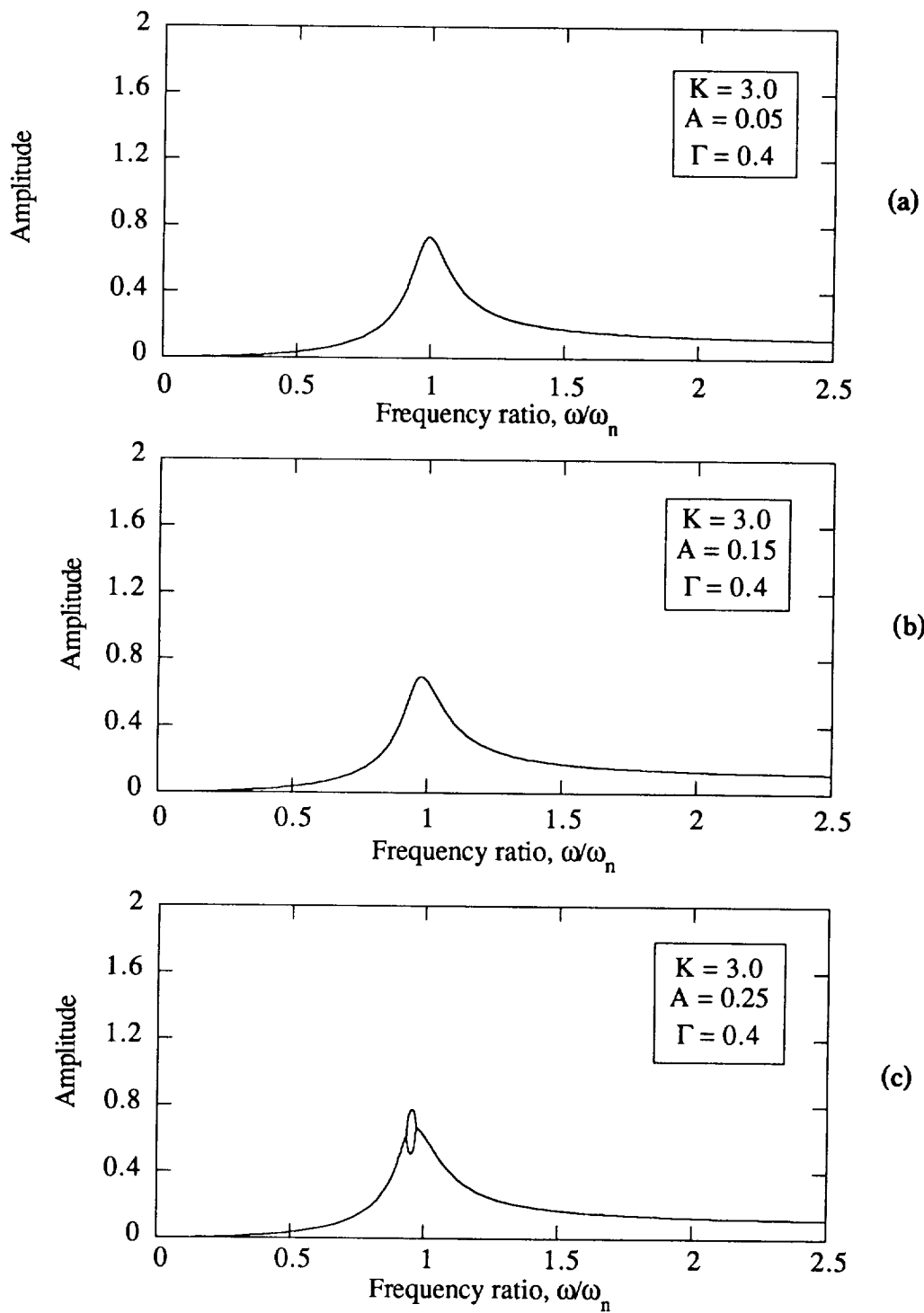
Figure 5. Effect of variation in coupling parameter A.
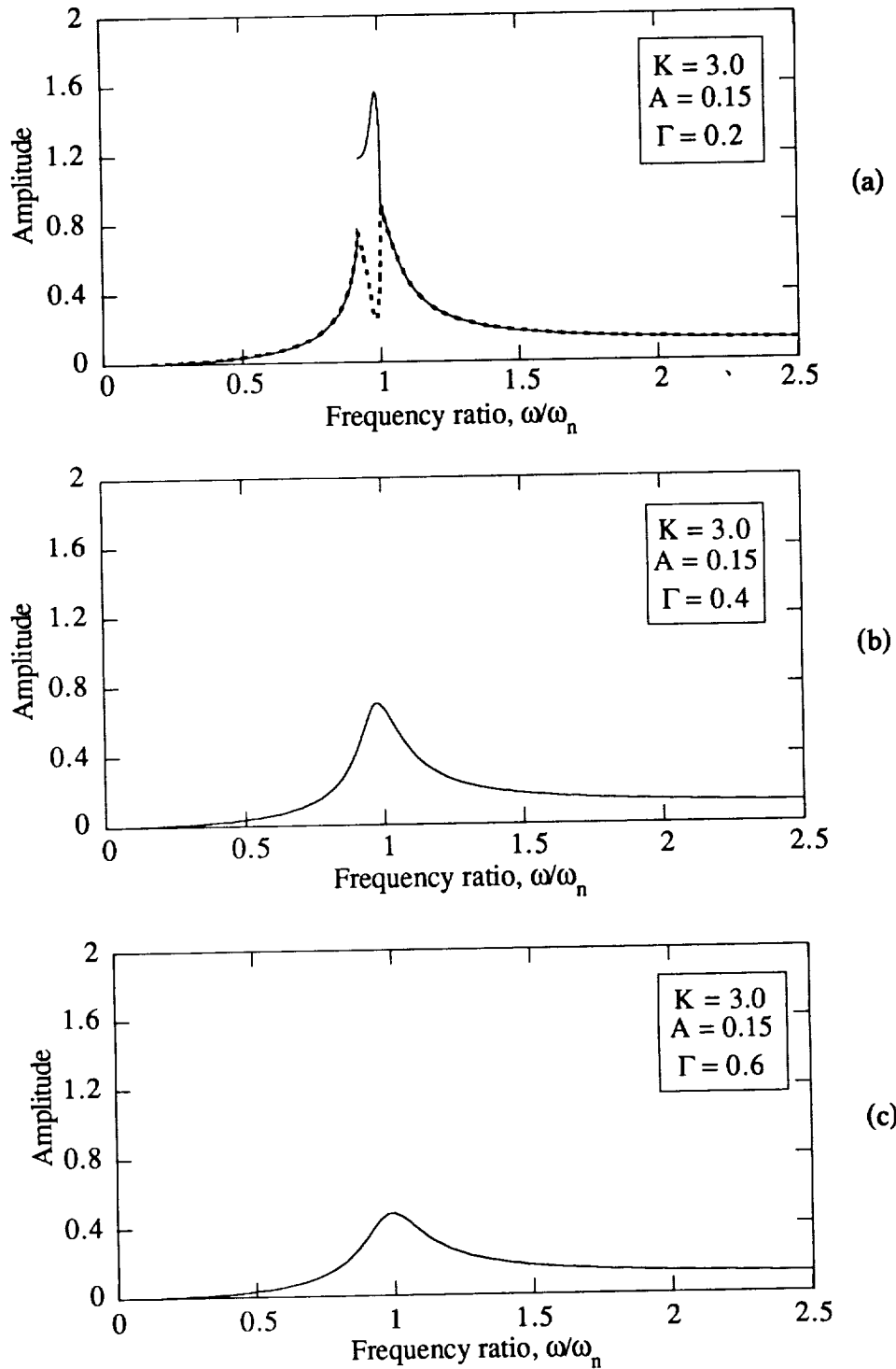
Figure 6. Effect of variation in derivative control coefficient Γ.
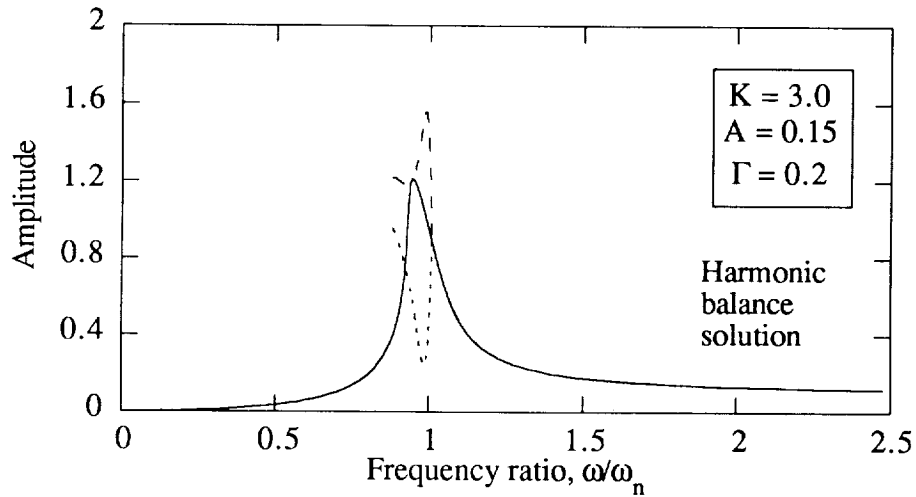
Figure 7. Multiple coexisting solutions by harmonic balance method.

The close correspondence between the numerical and analytical results supports the validity of both methods. Neither method alone is sufficient for a complete understanding, however, because the numerical solutions are dependent on initial conditions, and the analytical solutions provide no information on stability.

The numerical integration can in fact be used to track the unstable solutions to a very limited extent by careful choice of initial conditions, as shown in Figure 9 by the parts of the curves labelled "alternate solution". These initial conditions are based on the harmonic balance results, and tend further to support the validity of both methods.
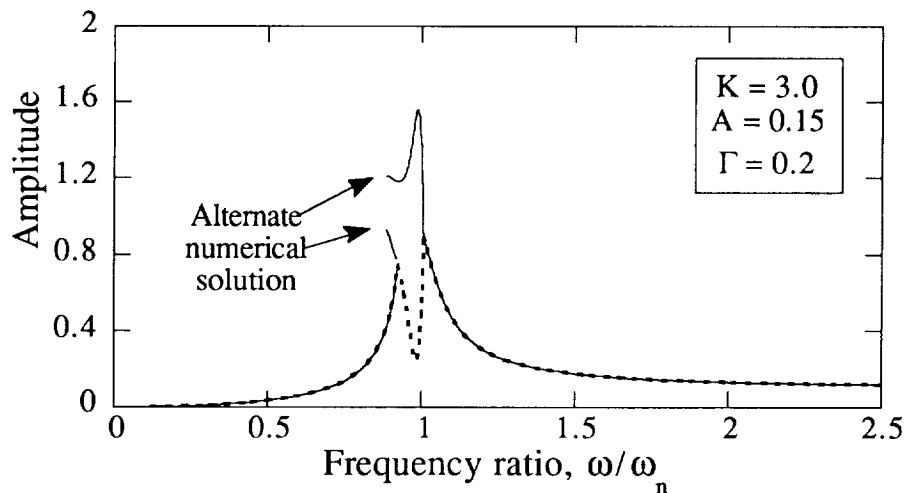
Figure 8. Limited unstable solution-following by numerical integration.

CONCLUSIONS

Equations of motion and limited parametric studies are presented for the case of a magnetic bearing subject to flux control, with geometric coordinate coupling. There are two effects of the coupling parameter on the system potential energy: a reduction of the principal stiffness, and introduction of a nonlinear normal stiffness.

The equations of motion are nonlinear and exhibit behavior that is distinctly different from that of linear systems. In forced response, the amplitudes of the system show bifurcations that are the result of changes in stability of multiple coexisting solutions. The stability seems mostly to be amplitude dependent, and the critical amplitude is a function of several parameters: K, Γ, and A.

In the long term, successful implementation of magnetic bearings where large eccentricities may be encountered will depend on a deeper understanding of the nonlinear characteristics of the combined rotor-actuator-control system.

REFERENCES

1. O'Connor, L. "Active Magnetic Bearings Give Systems a Lift'" Mechanical Engineering, V. 114, No. 7, pp. 52-57.

2. Williams, R. D., Keith, F. J., and Allaire, P. E., "A Comparison of Analog and Digital Controls for Rotor Dynamic Vibration Reduction through Active Magnetic Bearings," Journal of Engineering for Gas Turbines and Power, V. 113, No. 4, pp.535-543.

3. Lee, C. W., and Kim, J. S., "Modal Testing and Suboptimal Vibration Control of Flexible Rotor Bearing System by Using a Magnetic Bearing," Journal of Dynamic Systems, Measurement, and Control, V. 114, No. 2, pp. 244-252.

4. Nonami, K., Yamanaka, T., and Tominaga, M., "Vibration and Control of a Flexible Rotor Supported by Magnetic Bearings," JSME International Journal, Series III, V. 33, No. 4, pp. 475-482.

5. Knight, J. D., Xia, Z., and McCaul, E. B., "Forces in Magnetic Journal Bearings: Nonlinear Computation and Experimental Measurement," Proceedings of 3rd International Symposium on Magnetic Bearings, Alexandria, VA, 1992, P. E. Allaire, ed.

6. Walsh, T. F., "Nonlinear Dynamic Analysis of a Magnetic Bearing System with Flux Control: The Effects of Coordinate Coupling'" M. S. Thesis, Duke University, 1993.